International Journal of Pharmaceutics 493 (2015) 96–101

Contents lists available at ScienceDirect

International Journal of Pharmaceutics

journal homepage: www.elsevier.com/locate/ijpharm

^{131}I–Zn–Chlorophyll derivative photosensitizer for tumor imaging and photodynamic therapy

Kasim Ocakoglu[a,b,*], Ozge Er[c], Guven Kiyak[a], Fatma Yurt Lambrecht[c,**], Cumhur Gunduz[d], Cagla Kayabasi[d]

[a] Advanced Technology Research & Application Center, Mersin University, Ciftlikkoy Campus, TR-33343 Yenisehir, Mersin, Turkey
[b] Department of Energy Systems Engineering, Faculty of Technology, Mersin University, TR-33480 Tarsus, Mersin, Turkey
[c] Department of Nuclear Applications, Institute of Nuclear Science, Ege University, Bornova, 35100 Izmir, Turkey
[d] Department of Medical biology, Faculty of Medicine, Ege University, Bornova, 35100, Izmir, Turkey

ARTICLE INFO

Article history:
Received 15 May 2015
Received in revised form 15 July 2015
Accepted 16 July 2015
Available online 28 July 2015

Keywords:
Photodynamic therapy
Cancer
Biodistribution
^{131}I
Radiolabeling
Chlorophyll

ABSTRACT

In recent years, the photodynamic therapy studies have gained considerable attention as an alternative method to surgery, chemotherapy and radiotherapy which is commonly used to fight cancer. In this study, biological potentials of a benzyloxy bearing zinc(II) pheophorbide-a (Zn-PH-A) were investigated via *in vivo* and *in vitro* experiments. Zn-PH-A was labeled with ^{131}I with high efficiency (95.3 ± 2.7%) and its biodistribution studies were investigated on female Albino Wistar rats. The radiolabeled photosensitizer had been intravenously injected into the tail vein, and then the animals were sacrificed at 30, 60 and 120 min post injection. The percent of radioactivity per gram of organs (%ID/g) was determined. The radiolabeled Zn-PH-A showed high uptake in ovary. In addition, photodynamic therapy studies of the photosensitizer were conducted in EMT6, murine mammary carcinoma and HeLa, human cervix carcinoma cell lines. For the photodynamic therapy studies, the cells with Zn-PH-A were exposed to red light (650 nm) at the doses of 10–30 J/cm^2. The results showed that Zn-PH-A has stronger PDT effect in EMT6 than HeLa cell. Our present work demonstrates ^{131}I-labeled photosensitizer as a bifunctional agent (PDT and nuclear imaging) which could be improved in future by using EMT6 growing tumor in nude mice.

© 2015 Elsevier B.V. All rights reserved.

1. Introduction

Photodynamic therapy (PDT) is a promising novel therapeutic method for the treatment of certain types of cancer and premalignant lesions. Photosensitizers (PS) are used in PDT as a source of reactive oxygen species. They are able to absorb light efficiently in 400–700 nm regions. The light-activated PS creates free radicals and, in the presence of molecular oxygen, these radicals and singlet oxygen destroy cells in the tissue. Singlet oxygen is one of the most important reactive oxygen species in biological systems which play a pivotal role as an intermediate in PDT. Since the photosensitizer is a key compound used in PDT, numerous studies have been carried out to synthesize new ones which may lead better results in the tumor treatment with PDT (Josefhen and Boyle, 2008; Fadel et al., 2010; Garcia et al., 2011).

The metalation of the photosensitizer's core influences the photophysical properties of the compound. The characteristics of the PS depend on the type of metal which is used. Paramagnetic metals coordinated phthalocyanines (Pcs) have shown shortened triplet life times, resulting in variations in the triplet quantum yields while diamagnetic metallo-Pcs have demonstrated encouraging photophysical properties; high triplet quantum yields and efficient singlet oxygen generation (Ali and van Lier, 1999; Josefhen and Boyle, 2008; Ocakoglu et al., 2014a,b; Er et al., 2015). In particular, the zinc and cadmium derivatives have shown high triplet quantum yields. In several studies, zinc(II) phthalocyanine has been assessed as a second generation photosensitizer shows activity against certain tumors (Ali and van Lier, 1999; Josefhen and Boyle, 2008). Besides, its chemical purity and high singlet oxygen quantum yield, has absorption Q bands at longer wavelengths (around 670 nm) where there is maximum penetration of light into tissues (Ali and van Lier, 1999; Josefhen and Boyle, 2008; Fadel et al., 2010; Garcia et al., 2011).

On the other hand chlorophyll (Chl) derivative is sensitive to the type of metal ion centrally cheated by the Chl macrocycle for

* Corresponding author. Fax: +90 3243610153.
** Corresponding author. Fax: +90 2323886466.
E-mail address: kasim.ocakoglu@mersin.edu.tr (K. Ocakoglu).

http://dx.doi.org/10.1016/j.ijpharm.2015.07.047
0378-5173/© 2015 Elsevier B.V. All rights reserved.

tumor. Because the pharmacokinetics of Zn-substituted pheophorbide a (Zn-PH-A) is very different from those of the native Mg-derivative. In particular, Zn-PH-A has a longer retention time and reaches higher levels in the tumor (Jakubowska et al., 2013; Garcia et al., 2011; Ali and van Lier, 1999). This encouraged to us to investigate biopotential of Zn-PH-A derivative for PDT activity and nuclear imaging. In our study Zn-PH-A was synthesized and labeled with ^{131}I using iodogen method for investigating nuclear imaging potential as *in vivo* and responses of the two cell lines to the photodynamic effect of Zn-PH-A derivative were compared.

2. Material and method

2.1. Materials

Na^{131}I was supplied by the Department of Nuclear Medicine, Sifa University. LC–MS/MS analyses were performed using an Agilent 6460 Triple Quad LC–MS/MS (80% MeOH + 20% H_2O + formic acid, negative scan, 0.3 ml/min). Elemental analyses were performed on a LECO-CHNS-932 elemental analyser. ^{1}H NMR spectra were performed on a Bruker 400 MHz spectrometer using residual solvent peaks as internal standards. All chemicals used the *in vitro* studies were purchased from Biological Industries; all other chemicals were purchased from Merck. Iodogen was supplied by Sigma–Aldrich. Cell culture studies were performed in a Thermo MSC Advantage 1.2 Laminar Air Flow cabinet. An Olympus Japan Inverted light microscope was used for counting cells. A Thermo Multimode microplate reader was used to determine the IC_{50} values of cell cultures.

2.2. Synthesis of methyl 3-devinyl-3-{1′-(benzyloxy)-ethyl}13^2-demethoxycarbonylpheophorbide a (PH-A)

3-devinyl-3-{1′-(benzyloxy)-ethyl}13^2-demethoxycarbonyl pheophorbide a (PH-A) was prepared according to slightly modified literature procedures (Pandey et al., 2005; Ocakoglu et al., 2011). The crude product was purified by silica gel column chromatography using *n*-hexane: ethyl acetate (4:1) as an eluant to remove excess benzyl alcohol followed by hexane: ethyl acetate (1:1) (Pandey et al., 2005). 78 mg (65% yield), m.p. 112–114 °C. UV (THF) λ_{max}: 661 (0.67), 605 (0.13), 533 (0.16), 503 (0.17), 408 (1.42). ^{1}H NMR (400 MHz, $CDCl_3$) δ ppm: 9.76 (s, 1H, CH-5), 9.54 (s, 1H, CH-10), 8.56 (s, 1H, CH-20), 7.40-7.31 (m, 5H, ArH), 6.02 (q, *J*= 6.8 Hz, 1H, 3^1-H), 5.28 (d, *J* = 19.6 Hz, 1H, 13^2-CH_2), 5.13 (d, *J* = 19.6 Hz, 1H, 13^2-CH_2), 4.80 (dd, *J* = 2 Hz, 9.6 Hz, 1H, OCH_2Ar), 4.62 (dd, *J* = 4 Hz, 8 Hz, 1H, OCH_2Ar), 4.54–4.45 (m, 1H, 18-H), 4.35-4.28 (m, 1H, 17-H), 3.72 (q, *J* = 8.0, 2H, CH_2-8^1), 3.69 (s, 3H, $COOCH_3$), 3.61 (s, 3H, 12^1-CH_3), 3.37 (s, 3H, 2^1-CH_3), 3.18 (s, 3H, 7^1-CH_3), 2.76–2.63, 2.62–2.48, 2.40–2.19 (m, 1H + 1H + 2H, 17-CH_2CH_2), 2.12–2,02 (m, 3H, 3^1-CH_3), 1.83 (dd, 3H, *J*= 2.8 Hz, 4.4 Hz, CH_3-18^1), 1.71 (t, 3H, *J*= 7.6 Hz, CH_3-8^2), 0.43 (brs, 1H, NH), −1.71 (brs, 1H, NH). MS (EI): *m/z* $C_{41}H_{44}N_4O_4$for calc. $[M+H]^+$: 656.

2.3. Synthesis of methyl 3-devinyl-3-{1′-(benzyloxy)-ethyl}13^2-demethoxycarbonyl pheophorbide a zinc complex (Zn-PH-A)

Standard zinc metallation of PH-A was carried out according to the literature procedures (Pandit et al., 2013; Ocakoglu et al., 2014a, b). Zinc complex was purified by silica gel column chromatography using *n*-hexane: ethyl acetate (4:1) as an eluent. 87% yield. UV (THF) λ_{max}: 653 (0.91), 606 (0.20), 568 (0.13), 520 (0.09), 486 (0.08), 425 (1.23), 408 (0.86). ^{1}H NMR (400 MHz, $CDCl_3$) δ ppm: 9.62 (s, 1H, CH-5), 9.40 (s, 1H, CH-10), 8.42 (s, 1H, CH-20), 7.27-7.17 (m, 5H, ArH), 5.88 (q, *J* = 8 Hz, 1H, 3^1-H), 5.11 (d, *J* = 19.6 Hz, 1H, 13^2-CH_2), 5.02 (d, *J* = 19.6 Hz, 1H, 13^2-CH_2), 4.80 (dd, *J* = 2 Hz, 9.6 Hz, 1H, OCH_2Ar), 4.62 (dd, *J* = 4 Hz, 8 Hz, 1H, OCH_2Ar), 4.41–4.31 (m, 1H, 18-H), 4.21–4.13 (m, 1H, 17-H), 3.61 (q, *J* = 8.0, 2H, CH_2-8^1), 3.55 (s, 3H, $COOCH_3$), 3.41 (s, 3H, 12^1-CH_3), 3.24 (s, 3H, 2^1-CH_3), 3.04 (s, 3H, 7^1-CH_3), 2.64–2.50, 2.48–2.33, 2.26–2.05 (m, 1H + 1H + 2H, 17-CH_2CH_2), 2.03-1.98 (m, 3H, 3^1-CH_3), 1.71-1.65 (m, 3H, CH_3-18^1), 1.57 (t, *J* = 7.6 Hz, 3H, CH_3-8^2) (Scheme 1).

2.4. Radiolabeling of Zn-PH-A

The synthesized Zn-PH-A was dissolved in ethanol (1 mg/100 μl) and 100 μg Zn-PH-A was used in each radiolabeling study. Thin layer radio chromatography (TLRC) was performed by using cellulose-coated TLC plates and two solvent systems which are *n*-butanol–water–acetic acid (4–2–1) and chloroform–acetic acid (9–1), for quality control of radiolabeling.

2.5. Effect of pH on radiolabeling efficiency

The pH of the solution was adjusted to 3, 7 and 10 by using 1 MHCl/0.2 N NH_4OH after the 100 μg Zn-PH-A was diluted with distilled water (pH 5). Labeling with ^{131}I (250 μ Ci) was performed each pH and repeated 3 times. Afterwards, the radiolabeling yield was determined with TLRC method.

2.6. Effect of iodogen amount on radiolabeling efficiency

The studies regarding iodogen amount were performed after determination of optimum pH. In this study, 0.25, 0.5 and 1 mg amount of iodogen was used, and radiolabeling yield was determined with TLRC method.

2.7. In vitro stability studies

Labeling efficiency of the radiolabeled photosensitizer which was labeled under optimum conditions was determined at 30 min,

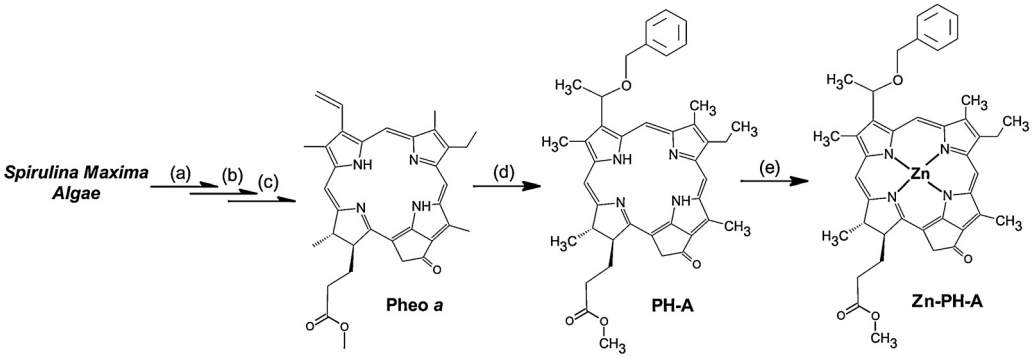

Scheme 1. Synthesis of methyl 3-devinyl-3-{1′-(benzyloxy)-ethyl}13^2-demethoxycarbonylpheophorbide a zinc complex (Zn-PH-A).

1, 2, 3 and 24 h via TLRC method for determining *in vitro* stability of radiolabeled photosensitizer.

2.8. Lipophilicity test of ^{131}I labeled Zn-PH-A

The partition coefficient was determined by mixing complex (100 μl) with an equal volume of *n*-octanol (3 ml) and water (3 ml) in a centrifuge tube. The mixture was mixed on a magnetic mixer for 1 h and then centrifuged at 2500 rpm for 5 min. 500 μl sample from each phase was pipetted and counted in a Cd(Te) RAD-501 single channel analyzer. The measurement was repeated three times. The partition coefficient was calculated.

2.9. Biodistribution study

The experiment was approved by the Animal Ethics Committee of Ege University. For biodistribution purpose, we used female albino Wistar rats weighing ~250 g. 0.3 ml of the radiolabeled photosensitizer (specific activity: 268.12 MBq/μmol/rat) was injected into the tail vein of anesthetized rats. Three rats were used for one set of experiments. After a definite time, the rats were sacrificed via anesthesia. After samples of liver, ovary, breast, and uterus were removed, they were weighed and the activity was measured using a Cd(Te) RAD-501 single channel analyzer. The results were expressed as the percent uptake of injected dose per gram tissue (%ID/g).

2.10. In vitro photosensitizing efficacy

EMT6 and HeLa cells were cultured in RPMI 1640 supplemented with 10% fetal bovine serum in 95% humidity with 5% CO_2. The cells were seeded in triplicate at 1×10^5 cells/well in 96-well plate. Cells were incubated overnight before adding the desired zinc phthalocyanine compound at variable concentrations (1.563–100.00 μM). After the 3 h incubation with the compound in the dark, cells were exposed to red light (666 nm) to deliver doses of 10–30 J/cm^2. After light treatment, fresh medium was added and the cells were incubated for 24 h. Phototoxicity was assessed after 24 h by comparing the growth of treated cells to control cells as measured by The water soluble tetrazolium salts (WST-1) method using a microplate reader (Varioskan Flash Multimode Reader-Thermo, Finland) at 450 nm three hours later. Then, the percentage of cytotoxicity was calculated.

3. Result and discussion

3.1. Quality control of radiolabeling Zn-PH-A

The labeling efficiency of Zn-PH-A was determined as 95.3 ± 2.7% at the optimum condition (1 mg iodogen, pH 5, room temperature, 30 min) using TLRC method. R_f values of $Na^{131}I$ and ^{131}I labeled Zn-PH-A were determined as 0.45 and 0.96 by TLRC respectively when mobile phase 1 (*n*-butanol/water/acetic acid, 4:2:1) was used. When mobile phase 2 (chloroform/acetic acid, 9:1) was used, the R_f values of $Na^{131}I$ and ^{131}I labeled Zn-PH-A were 0.05 and 0.97, respectively. In previous studies, a Cu–chlorophyll derivative photosensitizer was labeled with ^{124}I and showed quite high labeling yields (Pandey et al., 2005; Pandey et al., 2009). On the other hand Cu-PH-A and Ni-PH-A were labeled with ^{131}I with high yield also (Ocakoglu et al., 2014a,b; Er et al., 2015).

3.2. Effect of pH on radiolabeling efficiency

It was found with pH studies, radiolabeling yield was extremely low at pH 3 and 10. Although radiolabeling yield was higher than pH 3 and 10 at pH 7, it was not appropriate. However, radiolabeling yield at pH 5 can be seen in Fig. 1 was extremely high (94.6 ± 5.4%). In a study performed by <***>Ozge et al., Ni-PH-A was labeled with ^{131}I at pH 10 (Er et al., 2015). As seen in literature pH of radioiodination changes due to molecular structure (Ocakoglu et al., 2014a,b; Er et al., 2015).

3.3. Effect of iodogen amount on radiolabeling efficiency

The studies regarding iodogen amount performed at pH 5 were showed that 0.25 and 0.5 mg iodogen was not sufficient although ^{131}I was oxidized under these conditions. However, 1 mg iodogen was suitable for the study, and its radiolabeling efficiency was found to be 95.3 ± 2.7% (Fig. 2). Labeling with radioiodine is usually accomplished by electrophilic subsitution reaction into an aromatic ring in the molecule of interest. In this case oxidized iodine (I^+) can easily substitute with a hydrogen atom in benzene

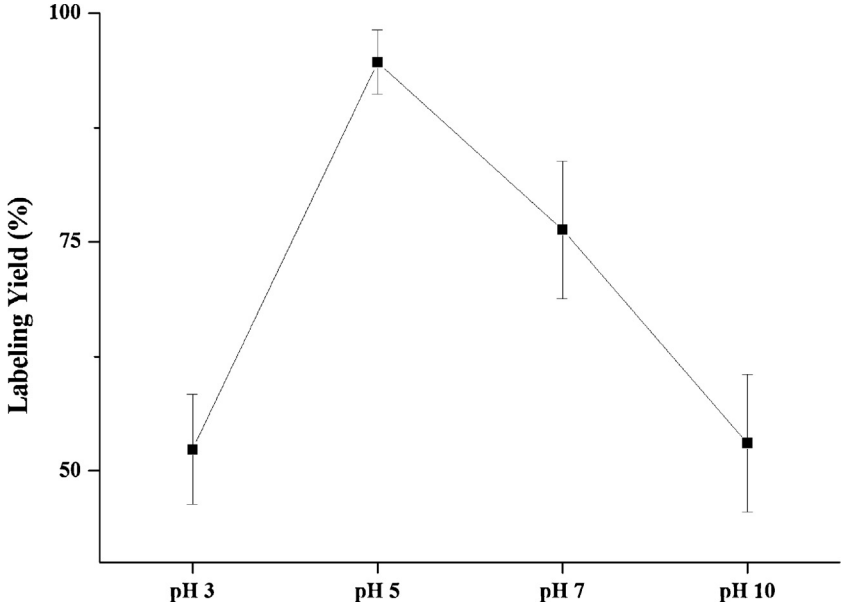

Fig. 1. Labeling yield of ^{131}I-Zn-PH-A at different pH values.

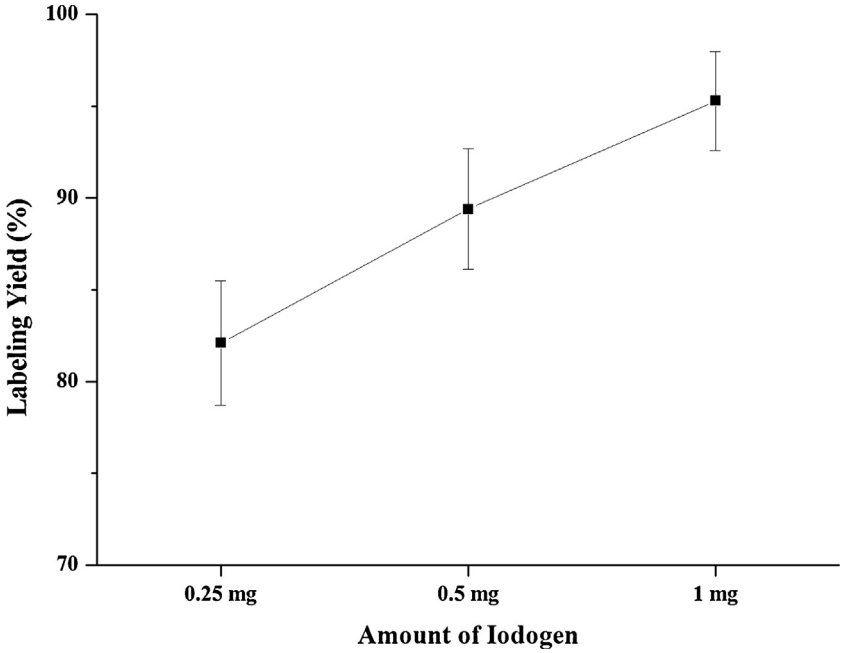

Fig. 2. Labeling yield of ^{131}I-Zn-PH-A at different amount of iodogen.

ring in order to generation iodine complex (Kowalsky and Perry, 1987; Yurt Lambrecht et al., 2006; Seyitoglu et al., 2009; Bayrak et al., 2010; Ocakoglu et al., 2014a,b; Er et al., 2015).

3.4. In vitro *stability studies*

The complex was found to be stable in *in vitro* conditions. While radiolabeled efficiency for 30 min was found to be 98.0 ± 1.0%, radiolabeled yield at the end of 1440 min decreased to 94.3 ± 1.2% (Fig. 3). The results showed that ^{131}I-Zn-PH-A has enough shelf life for imaging study like radioiodinated Cu-PH-A and Ni-PH-A (Ocakoglu et al., 2014a,b; Er et al., 2015).

3.5. *Lipophilicity test of ^{131}I labeled Zn-PH-A*

The partition coefficient of the complex was 2.7 ± 0.9. In the study related to ^{131}I-Ni-PH-A, lipophilicity of radiolabeled compound was found 2.07 ± 0.24 (Er et al., 2015). As seen ^{131}I-Ni-PH-A is lipophilic like ours.

3.6. *Biodistribution results*

The organ distribution of ^{131}I labeled Zn-PH-A expressed as percentage of injected dose per gram tissue in rats, 30, 60 and 120 min after intravenous administration is presented in Fig. 4. The

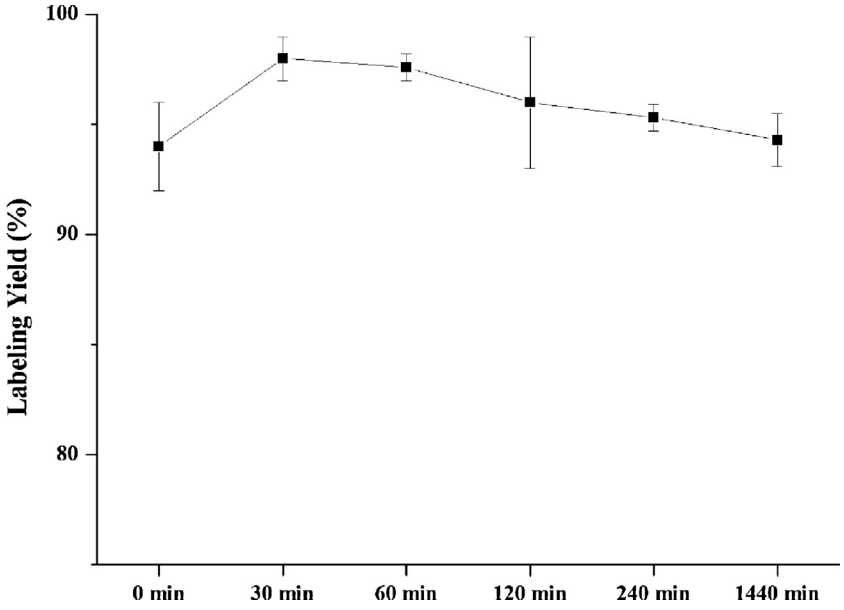

Fig. 3. In vitro stability of ^{131}I labeled Zn-PH-A at different times after labeling.

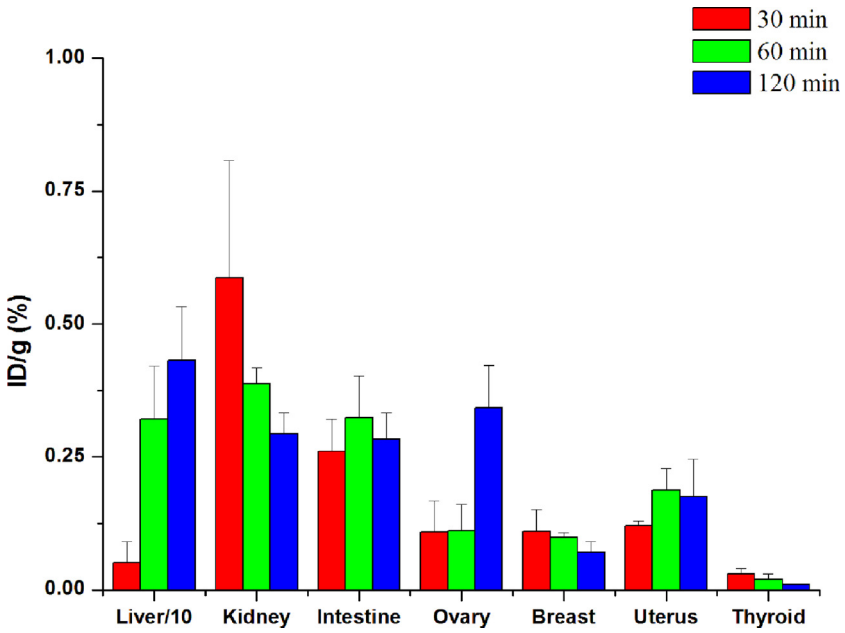

Fig. 4. Biodistribution results of ^{131}I labeled Zn-PH-A

uptake of ^{131}I-Zn-PH-A was slowly distributed after intravenous injection as shown by the renal and hepatobiliary elimination, although liver, intestine and kidney uptakes were significant. The maximum uptakes were reached in liver (%ID/g: 4.32 ± 0.61 at 120 min), intestine (%ID/g: 0.32 ± 0.08 at 60 min) and kidney (%ID/g: 0.59 ± 0.22 at 30 min). The uptake in intestine and kidney decreased with time. On the other hand the highest uptake of ^{131}I labeled Cu-PH-A in the liver (%ID/g: 4.0 ± 0.08) was found at 60 min by Ocakoglu et al. (2014a,b). Er et al. observed that ^{131}I labeled Ni-PH-A in the liver (%ID/g: 4.8±1.6) reached maximum value at 30 min (Er et al., 2015). As seen in these studies radioiodinated metalo-PS have similar uptakes in liver. On the other hand, the thyroid gland was controlled, and its activity was found to be low. It was observed that ^{131}I labeled Zn-PH-A was stable *in vivo* against biological decomposition.

We determined the highest uptakes (%ID/g) in ovary at 120 min, breast at 30 min and uterus at 60 min which were 0.34± 0.08, 0.11±0.04, 0.19±0.04, respectively. While the uptake of ^{131}I-Cu-PH-A was maximum in ovary at 60 min (%ID/g: 0.13), breast at 30 min ((%ID/g: 0.06) and uterus at 30 min (%ID/g: 0.05)), the highest uptake of ^{131}I-Ni-PH-A were 0.58 at 30 min for ovary, 0.12 at 30 min for breast and 0.13 at 30 min for uterus (Ocakoglu et al., 2014a,b; Er et al., 2015). These data show the uptake in these organs changed a little bit. This change might be depending on metal atom in metalo-PS. Besides Ozgur et al. reported that the maximum uptake of ^{99m}Tc-PH-A-BSANPS in the breast and uterus was at 120 min. Otherwise the uptake of ^{99m}Tc-PH-A was found to be high in the ovary and uterus at 120 min and in the breast at 60 min. Our results display that ^{131}I labeled Zn-PH-A has higher uptake in the ovary at 120 min, like ^{99m}Tc-PH-A.These results could be the consequence of the presence of the zinc atom (Ozgur et al., 2012). It was depicted that many analogous photosensitizers, *i.e.*, ^{99m}Tc-PH-A-BSANPS, ^{99m}Tc-PH-A, and ^{99m}Tc-HP, PH-A (such as T3, 4BCPC, and Photosan-3) are removed from body via the urinary system (Aprahamian et al., 1993; Murugesen et al., 2002; Yang et al., 2010; Ocakoglu et al., 2011; Ozgur et al., 2012). On the other hand, it has been reported by Pandey et al. that ^{124}I PS shows high accumulation in the liver and kidney at 24 h post-injection. Pandey et al. postulated that the high affinities of these compounds for the liver could be a result of their higher lipophilicity (Pandey et al., 2005). The lipophilicity of our compound is obtained as 2.7 ± 0.9 which is similar with the literature results and may be an advantage for imaging.

Several strategies for better delivery of the photosensitizers have been suggested, like utilization of photosensitizer-conjugated nanoparticles or positive effects of metal ions as potential carrier vehicles. The studies have shown that the presence of the metal ion in a photosensitizer affects the uptake of the photosensitizer and/or the molecule used for labeling, which increases its biological potential (Josefhen and Boyle, 2008; Ali and van Lier, 1999). As a result radiolabeled Zn-PH-A uptake is higher also in ovary compared with ^{99m}Tc-PH-A. It is possible to effect of metal which is binding in central of PH-A.

3.7. In vitro *photosensitizing efficacy*

IC_{50} doses of Zn-PH-A were found as 1.10 μM in EMT6 cells and as 2.44 μM in HeLa cells. The photosensitizing efficiency of Zn-PH-A was analyzed at 1.56 μM and three different light doses (10, 20 and 30 J/cm^2). The results indicated that Zn-PH-A was more effective in EMT6 cell with the light dose of 20 J/cm^2 (Figs. 5 and 6). When using 1.56 μM Zn-PH-A and 20, 30 J/cm^2 light dose, EMT6 cell viability decreased 19 and 12%, respectively.

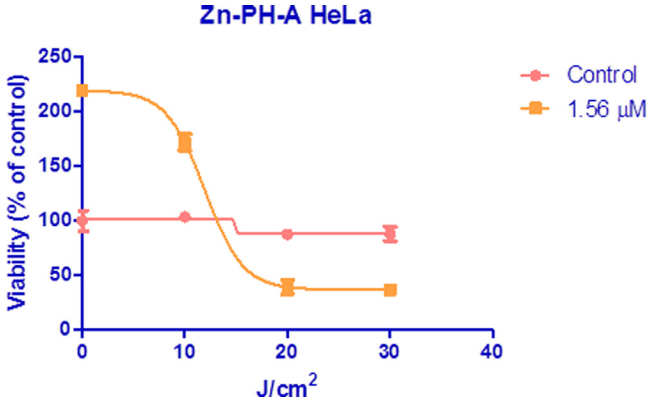

Fig. 5. *In vitro* photosensitizing activity of 1.56 μM Zn-PH-A in HeLa cells with the light doses of 10, 20 and 30 J cm^{-2}.

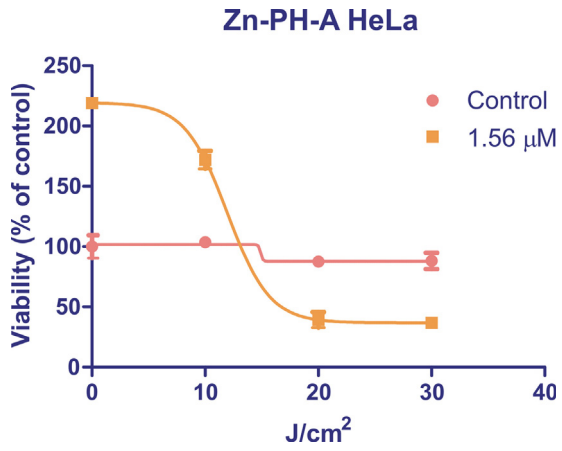

Fig. 6. *In vitro* photosensitizing activity of 1.56 μM Zn-PH-A in EMT6 cells with the light doses of 10, 20 and 30 J cm^{-2}.

The phototoxicity of ZnPc and ZnF16Pc in the three liposomal formulations was studied in HeLa cell lines by Garcia et al. In this study the dye aggregation degree in the liposome affects its photodynamic activity was assessed. They obtained using ZnPc show substantial differences among the liposomes employed, particularly in cell viability measured after irradiation (Garcia et al., 2011). Jakubowska et al., reported that Zn-PH-A causes a high PDT effect at low concentration and light an A549 cell line. They suggested Zn-PH-A showed the strongest PDT effect compared with its Mg analog and photofrin which are not including zinc atom (Jakubowska et al., 2013). In literature it is depicted that Zn atom increases PDT effect (Jakubowska et al., 2013; Garcia et al., 2011; Ali and van Lier, 1999). Our results showed that Zn-PH-A has strong PDT potential on EMT6 cell.

4. Conclusions

In the present study, the biodistribution of ^{131}I labeled Zn-PH-A in healthy female rats indicated high uptake in the liver uterus and ovary. In addition, Zn-PH-A demonstrated the strongest PDT effect in EMT6 cell line at low dose and low light dose. In conclusion, the obtained results show that radiolabeled Zn-PH-A might be useful for ovary tumors and promising effective photosentizing agent for PDT.

Acknowledgement

The authors gratefully acknowledge financial support by The Scientific and Technological Research Council of Turkey, TUBITAK (Grant no: 112T565).

References

Ali, H., van Lier, J.E., 1999. Metal complexes as photo- and radio-sensitizers. Chem. Rev. 99 (9), 2379–2450.
Aprahamian, M., Evrard, S., Keller, P., Tusuji, M., Balboni, G., Damgè, C., Marescaux, J., 1993. Distribution of pheophorbide A in normal tissues and in an experimental pancreatic cancer in rats. Anticancer Drug Des. 8 (2), 101–114.
Bayrak, E., Yurt Lambrecht, F., Durkan, K., Yilmaz, O., 2010. In vitro evaluation, biodistribution in rats of radiolabeled raloxifene. J. Appl. Radiat. Isot. 68, 33–36.
Er, O., Yurt Lambrecht, F., Ocakoglu, K., Kayabasi, C., Gunduz, C., 2015. Primary evaluation of a nickel-chlorophyll derivative as a multimodality agent for tumor imaging and photodynamic therapy. J. Radioanal. Nucl. Chem. doi:http://dx.doi.org/10.1007/s10967-015-4081-x.
Fadel, M., Kassab, K., Fadeel, D.A., 2010. Zinc phthalocyanine-loaded PLGA biodegradable nanoparticles for photodynamic therapy in tumor-bearing mice. Lasers Med. Sci. 25, 283–292.
Garcia, A.M., Alarcon, E., Mūnoz, M., Scaiano, J.C., EdwardsA, M., Lissi, E., 2011. Photophysical behaviour and photodynamic activity of zinc phthalocyanines associated to liposomes. Photochem. Photobiol. Sci. 10, 507.
Jakubowska, M., Szczygiel, M., Michalczyk-Wetula, D., Susz, A., Stochel, G., Elas, M., Fiedor, L., Urbanska, K., 2013. Zinc-pheophorbide a—higly efficient low-cost photosensitizer against human adenocarsinoma in cellular and animal models. Photodiagn. Photodyn. Ther. 10, 266–277.
Josefhen, L.B., Boyle, R.W., 2008. Photodynamic Therapy and the Development of Metal-Based Photosensitisers. Hindawi Publishing Corporation article. ID 276,109.
Kowalsky, R.C., Perry, J.R., 1987. Radiopharmaceuticals in Nuclear Medicine Practice, vol. 91. Appleton & Lange, A Publishing Division of Prentice-Hall, United States of America.
Murugesen, S., Shetty, S.J., Srivastava, T.S., Samuel, A.M., Noronha, O.P., 2002. Preparation and biological evalution of the new chlorin photosensitizer T3, 4BCPC for detection and treatent of tumors. J. Photochem. Photobiol. B 68 (1), 33–38.
Ocakoglu, K., Er, O., Yurt Lambrecht, F., Yılmaz Susluer, S., Kayabasi, C., Gunduz, C., Yılmaz, O., 2014a. Evaluation of cancer imaging potential and photodynamic therapy efficacy of copper(II) benzyloxypheophorbide-a. J. Drug Target 1–7 Early Online.
Ocakoglu, K., Joya, K.S., Harputlu, E., Tarnowska, A., Gryko, D.T., 2014b. Nanoscale bio-inspired light-harvesting system develop from self-assembled alkyl-functionalized metallochlorins nano-aggregates. Nanoscale 6, 9625–9631.
Ocakoglu, K., Bayrak, E., Onursal, M., Yilmaz, O., Lambrecht, F.Y., Holzwarth, A.R., 2011. Evaluation of 99mTc-pheophorbide-a use in infection imaging: a rat model. Appl. Radiat. Isot. 69, 1165–1168.
Ozgur, A., Lambrecht, F.Y., Ocakoglu, K., Gunduz, C., Yucebas, M., 2012. Synthesis and biological evaluation of radiolabeled photosensitizer linked bovine serum albumin nanoparticles as a tumor imaging agent. Int. J. Pharm. 422, 472–478.
Pandey, S.K., Gryshuk, A.L., Sajjad, M., Zheng, X., Chen, Y., Abouzeid, M.M., Morgan, J., Charamisinau, I., Nabi, H.A., Oseroff, A., Pandey, R.K., 2005. Multimodality agents for tumor imaging (PET, Fluorescence) and photodynamic therapy. A possible see and treat approach. J. Med. Chem. 48, 6286–6295.
Pandey, S.K., Sajjad, M., Chen, Y., Pandey, A., Missert, J.R., Batt, C., Yao, R., Nabi, H.A., Oseroff, A.R., Pandey, R.K., 2009. Compared to purpurinimides, the pyropheophorbide containing an iodobenzyl group showed enhanced PDT efficacy and tumor imaging (124I-PET) ability. Bioconjugate Chem. 20, 274–282.
Pandit, A., Ocakoglu, K., Buda, F., van Marle, T., Holzwarth, A.R., de Groot, H.J.M., 2013. structure determination of a bio-inspired self-assembled light-harvesting antenna by solid-state NMR and molecular modeling. J. Phys. Chem. B 117, 11292–11298.
Seyitoglu, B., Yurt Lambrecht, F., Durkan, K., 2009. Labeling of apigenin with 131I and bioactivity of 131I-apigenin in male and female rats. J. Radioanal. Nucl. Chem. 279 (3), 867–873.
Yang, S.G., Chang, J.E., Shin, B., Park, S., Na, K., Shim, C.K., 2010. 99mTc-hematoporphyrin linked albumin nanoparticles for lung cancer targeted photodynamic therapy and imaging. J. Mater. Chem. 20, 9042–9046.
Yurt Lambrecht, F., Durkan, K., Yıldırım, Y., Acar, Ç., 2006. Labeling of acetaminophen with I-131 and biodistribution in rats. Chem. Pharm. Bull. 54 (2), 245–247.